Proceedings of the ASME 2022
International Design Engineering Technical Conferences and
Computers and Information in Engineering Conference
IDETC/CIE2022
August 14-17, 2022, St. Louis, Missouri

DETC2022-XXXX

DESIGN OF DECOUPLED AND DYNAMICALLY ISOTROPIC PARALLEL MANIPULATORS WITH FIVE DEGREES OF FREEDOM

Yogesh Pratap Singh
Dept. of Mechanical Engineering
Indian Institute of Science
Bangalore, India

Ashitava Ghosal
Dept. of Mechanical Engineering
Indian Institute of Science
Bangalore, India

ABSTRACT

A six degree of freedom (DOF) two-radii Gough-Stewart Platform (GSP) can be designed to be dynamically isotropic and has been proposed for micro-vibration isolation. In many applications, the torsional mode can be ignored, and a 5-DOF dynamically isotropic, parallel manipulator capable of attenuating three translational (3T) and two rotational (2R) modes are sufficient. In this work, we present the design of a novel two radii, 5-DOF dynamically isotropic parallel manipulator, which can be used for vibration isolation purposes where the torsion mode can be ignored. We present closed-form solutions in their explicit form to this design problem, and these are obtained using a geometry-based approach. The first design is based on a modification to the two radii GSP and provides enhanced design flexibility and feasibility. The second design of a decoupled 5-DOF GSP is based on superposing two 3-DOF dynamically isotropic or decoupled parallel manipulators, which are the well-known 3-3 RPS parallel manipulators. The closed-form solutions for these 3-DOF isotropic designs are obtained. It is shown that the 5-DOF decoupled design have two translational modes, namely the (X, Y) modes, which are decoupled from two rotational modes (Rot(X), Rot(Y)) and are controlled by two different sets of three struts. This feature can lead to simpler control and less power requirements if active vibration control is chosen. The designs presented in this work include the effect of asymmetricity and payload's centre of mass variation in the moving platform. The dynamically isotropic and decoupled designs obtained were successfully validated using the finite element software ANSYS®.

Keywords: Dynamic isotropy, Decoupling, Gough-Stewart Platform, Natural frequency matrix, Degree of freedom

1. INTRODUCTION

Precise micro-motion parallel manipulators (PM) are a current topic of interest for industries due to their wide range of applications, including chip assembly in the semiconductor industries, vibration isolation for space applications, small parts precision machining, cell manipulation in biotechnology, and precise surgery [1-4]. These micro-motion PMs offer several advantages over their serial counterparts, such as lower inertia, improved dynamic behaviour, better payload capacity, greater stiffness, high speed, and increased reliability and repeatability [1]. The major disadvantage of a general PM includes limited workspace and complex control algorithm [1]. Precise micro-motion PMs do not suffer from this drawback owing to their low workspace requirements. On the other hand, the use of a dynamically isotropic or a decoupled configuration simplifies control, and a decoupled control strategy can be used as a multi-input-multi-output (MIMO) system is ideally converted into several single-input-single-output (SISO) systems [5]. Additionally, dynamic isotropy implies that the first six natural frequencies are ideally the same, which is a primary design consideration for designing a micro-vibration isolator [2-4]. In such an ideal design, the region of isolation corresponding to a particular DOF (degree of freedom) will not be affected by the peak associated with the cross DOFs in the amplitude vs. frequency curve. Moreover, it is easy to tune a damper for a particular bandwidth, given all resonance peaks lie close to each other [3,4]. An isotropic manipulator is superior in kinematic accuracy and does not have singular configurations [6].

Most of the previous works on decoupling or dynamic isotropy configuration have been confined to 6-DOF 6-6 Gough-Stewart platforms (GSPs) [2,3,4,5,7-11]. Literature states that a conventional GSP cannot give static isotropy [11] and it also fails to give dynamic isotropy. However, dynamic isotropy can be achieved using a two radii GSP or a modified GSP (MGSP). It differs from the conventional 6-6 GSP with the anchor points described on two radii on each platform instead of one radius in a traditional GSP, as shown in Fig. 1. Along the same lines, researchers also proposed the dynamic isotropy concept in GSPs with more than six active legs [4,12]. However, there are many applications where the 6-DOF is not necessarily required [1,13,14]. For example, most machining operations require a maximum of 5 DOFs [1]. In the context of the micro-vibration isolation, the rotating or reciprocating component may induce disturbance only along some specific directions, indicating a requirement for less than 6-DOF isolators. Therefore, the study of dynamically isotropic conditions for limited DOF manipulators remains a novel area for research. These limited DOF manipulators are more economical due to the requirements of fewer actuators [13]. In space application, this would significantly reduce power consumption. Due to their simplified mechanical structure, the manufacturing cost will also be lower for manipulators with less DOF [13]. With the motivation of utilizing advantages associated with a limited DOF PM as well as with a decoupled/isotropic design, we investigated dynamic isotropy and decoupling in applications requiring three and five DOF precise micro-motion applications.

Five DOF manipulators in terms of mobility can be classified as 3R2T [15,16] or 2R3T [14,17] type (R denotes a rotational DOF, and T denotes a translational DOF). Piccin et al. in [17] proposed a 5-DOF (2R3T) parallel mechanism for the diagnosis and therapy of tumors in the context of interventional radiology. Maurin et al. in [18] built a 5-DOF robotic device to help practitioners perform accurate needle insertion while preserving them from harmful intra-operative X-rays imaging devices. Along similar lines, this paper first presents a closed-form solution for a 5-DOF (2R3T) dynamically isotropic design in a two radii GSP. The isotropic design and solutions are more straightforward and mechanically feasible than a 6-DOF isotropic two radii GSP design presented in our previous work [3,4]. Solutions to another class of novel decoupled 5-DOF GSPs are obtained by geometrical superposition of two 3-DOF isotropic and decoupled parallel manipulators containing rotary (R), prismatic (P), and spherical (S) joints; one with isotropy in three translational DOFs (3T) and the other with isotropy about the $\boldsymbol{X}$, $\boldsymbol{Y}$ rotations and along the $\boldsymbol{Z}$ translation (2R1T). In these special 5-DOF designs, the two rotational DOFs (about $\boldsymbol{X}$ and $\boldsymbol{Y}$) are uncoupled from two translational DOFs (along $\boldsymbol{X}$ and $\boldsymbol{Y}$). This means that only three struts need to be actuated for motion along any of these uncoupled DOF while other struts remain passive. While all the previous literature has discussed only 6-6 conventional GSP or two radii GSP, which have rotational symmetry (equal angular spacing of mounting points along the circumference, typically 120°), this paper extends to three and four radii GSPs which do not show rotational symmetry. To the best of our knowledge, closed-form solutions to such configurations are not available in literature for unsymmetrical GSPs. The variation of the payload's center of mass (COM) from the top platform is considered in all our formulations.

To arrive at the above-mentioned superposed design, dynamic isotropy in 3-DOF PMs is first investigated in both 3T and 2R1T configurations. Despite being a commonly studied manipulator (see for example [19-21]), the application of 2R1T remains limited since it can have only two orientation and one translational degrees of freedom [20]. The 3-DOF, 3-3 RPS parallel manipulators, can also show pure translational motions for a specific point in an arrangement where all struts meet at the payload's COM and the dynamic isotropy with this specific geometry is also examined in this work. These 3-DOF PMs with pure translational motion have a potentially wide range of applications [13]. This work is also extended to include asymmetric 3-3 RPS PMs to enhance the design flexibility.

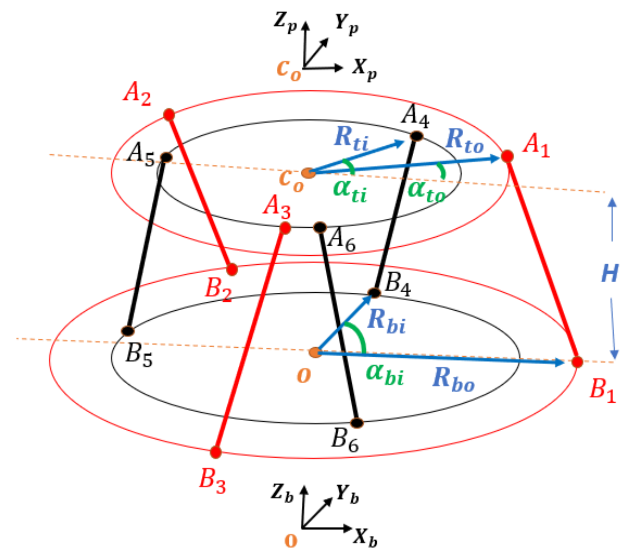

FIGURE 1: TWO RADII MODIFIED GOUGH-STEWART PLATFORM

2. 5-DOF DYNAMICALLY ISOTROPIC TWO RADII GSP (MGSP)

2.1 Nomenclature

Two radii Gough-Stewart Platform (MGSP) is a parallel manipulator with a movable top platform (payload mounted on it), a fixed base, and six struts with a prismatic actuator between them, as shown in Fig. 1. The anchoring points are on two radii and there are two sets of struts with three struts of equal lengths in each set. These struts have rotational symmetry of 120° angle along the circumference. The variables R_{bi} and R_{bo} are used to denote the inner and outer radii of the bottom platform, respectively. Similarly, R_{ti} and R_{to} represent the inner and outer radii of the top platform. The co-ordinates of a point on the base frame $\{B\}$ are represented by $\{x_b, y_b, z_b\}$ and on the top or moving frame $\{P\}$ are represented by $\{x_p, y_p, z_p\}$. The vector $\boldsymbol{oB_1}$ (magnitude equal to R_{bo}) is chosen along $\boldsymbol{X_b}$. The angle α_{bi}, α_{to}, α_{ti} are angles made by vectors $\boldsymbol{oB_4}, \boldsymbol{c_oA_1}, \boldsymbol{c_oA_4}$ with $\boldsymbol{X_b}$, respectively. The symbol H denotes the height between the two platforms. The struts are assumed to have a prismatic actuator (joint) connected to the top platform through a spherical joint and to the bottom platform through a spherical or a universal joint.

2.2 Formulation

The use of the Jacobian matrix [5,7,9,10,12] or a force transformation matrix [3,4,8] for GSPs at their neutral position is a reasonable assumption for precise micro motion PM, where the motion of the top platform is very small (e.g., micro-vibration isolation). The force transformation matrix ($[\mathbf{B}]$) is the transpose of the inverse Jacobian ($[\mathbf{J}]$) and is given by $[\mathbf{B}] = ([\mathbf{J}]^{-1})^T$. In this paper, we use the force transformation matrix to develop simple closed-form expressions for dynamic isotropy. Each platform is assumed to be a rigid body. All six struts are assumed to have an axial stiffness k (joint space). Hence, the stiffness matrix $[\mathbf{K_T}]$ in the task space is described as

$$[\mathbf{K_T}] = k[\mathbf{B}][\mathbf{B}]^T \quad (1)$$

Considering the payload's COM variation in the loop closure equation for the loop OBAP as shown in Fig. 2, the force transformation matrix (dimension 6×6 for the MGSP) can be derived [3] as

$$[\mathbf{B}] = \begin{bmatrix} \boldsymbol{s_1} & \cdots & \boldsymbol{s_6} \\ ({}^B[\mathbf{R}]_P({}^P\boldsymbol{p_1} - {}^P\boldsymbol{H_c})) \times \boldsymbol{s_1} & \cdots & ({}^B[\mathbf{R}]_P({}^P\boldsymbol{p_6} - {}^P\boldsymbol{H_c})) \times \boldsymbol{s_6} \end{bmatrix} \quad (2)$$

where, $\boldsymbol{s_j} = \dfrac{{}^B\boldsymbol{t} + {}^B[\mathbf{R}]_P{}^P\boldsymbol{p_j} - {}^B\boldsymbol{b_j}}{l_j}$ for $j=1,\ldots,6$

The vectors $\boldsymbol{s_j}$ are unit vectors along each leg. The vector ${}^B\boldsymbol{t}$ is the vector joining the center of the top and bottom platforms, $\boldsymbol{S_j}\,(= l_j\boldsymbol{s_j})$ is a vector along the respective leg of an MGSP with length l_j, and ${}^P\boldsymbol{p_j}$ and ${}^B\boldsymbol{b_j}$ are vectors locating the connecting points on the top and base platform expressed in their respective frames. For the neutral position of an MGSP, ${}^B[\mathbf{R}]_P = [\mathbf{I}]$ and ${}^B\boldsymbol{t} = [0\ 0\ H]^T$ and ${}^P\boldsymbol{H_c} = [0\ 0\ Y]^T$. The variable Y is the height of the payload's COM from the top platform along $\boldsymbol{Z_p}$ direction in Fig. 1. We are assuming that payload's COM, the center of the top platform, and the center of the bottom platform lie on the same vertical line. Precise micro motion PM operates around this neutral point. At this neutral point, $[\mathbf{B}]$ is a constant matrix. Given a Jacobian or force transformation matrix, the connection points on the payloads are not uniquely determined [4,10,11] and we can have an infinite number of configurations/solutions with the same $[\mathbf{J}]$ or $[\mathbf{B}]$ matrix.

Let $[\mathbf{M}]$ (dimension 6×6) be the payload's mass/inertia matrix in the task space. A diagonal structure of the $[\mathbf{M}]$ matrix can be obtained by choosing the coordinate system to coincide with the orientation of the principal axes of the payload. Hence, we can write:

$$[\mathbf{M}] = \mathrm{diag}\big([m_p\ m_p\ m_p\ I_{xx}\ I_{yy}\ I_{zz}]\big) \quad (3)$$

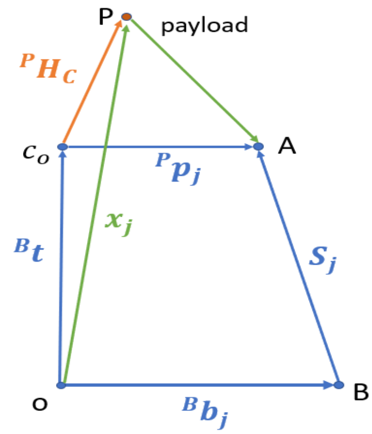

FIGURE 2 : A CLOSED LOOP FOR MGSP

where, m_p represents the payloads' mass and I_{xx}, I_{yy}, and I_{zz} represents its moment of inertia along each direction with respect to its COM. From $[\mathbf{M}]$ and $[\mathbf{K_T}]$, and using Eq. (1), the natural frequency matrix $[\mathbf{G}]$ in the task space [3,4,7,9,10] is given by

$$[\mathbf{G}] = [\mathbf{M}]^{-1}[\mathbf{K_T}] = [\mathbf{M}]^{-1}k[\mathbf{B}][\mathbf{B}]^T \quad (4)$$

For dynamic isotropy in the 5-DOF application (2R3T type with torsional mode ignored), the first five eigenvalues of the natural frequency matrix must be equal. Using Eqs. (2), (3), and (4), the $[\mathbf{G}]$ matrix is obtained as:

$$[\mathbf{G}] = \begin{vmatrix} \mathbf{P} & \mathbf{T} \\ \mathbf{T}^T & \mathbf{U} \end{vmatrix} \quad (5)$$

$$[\mathbf{P}] = \mathrm{diag}(\lambda_1, \lambda_2, \lambda_3)\,, [\mathbf{U}] = \mathrm{diag}(\lambda_4, \lambda_5, \lambda_6)$$

$$[\mathbf{T}] = \begin{bmatrix} \mu_{11} & -\mu_{12} & 0 \\ \mu_{12} & \mu_{11} & 0 \\ 0 & 0 & \mu_{33} \end{bmatrix}$$

The expressions for the λ's and μ's are given in Appendix section (see Eqs. (A1)).

There are two sets of struts with lengths l_1 and l_2 related to each other by a leg length ratio (a) and expressed as:

$$l_2 = al_1 \quad (6)$$

where

$$l_1 = |\boldsymbol{S_1}| = |\boldsymbol{S_2}| = |\boldsymbol{S_3}| = \sqrt{R_{to}^2 + R_{bo}^2 - 2R_{to}R_{bo}\cos(\alpha_{to}) + H^2}$$

$$l_2 = |\boldsymbol{S_4}| = |\boldsymbol{S_5}| = |\boldsymbol{S_6}| = \sqrt{R_{ti}^2 + R_{bi}^2 - 2R_{ti}R_{bi}\cos(\alpha_{bi} - \alpha_{ti}) + H^2}$$

If ω denotes the natural frequency of the MGSP, then for 5-DOF dynamic isotropy, the following conditions needs to be satisfied:

$$\begin{gathered}\lambda_1 = \lambda_2 = \lambda_3 = \lambda_4 = \lambda_5 = \omega^2 \\ \lambda_6 = 0 \\ \mu_{11} = \mu_{12} = \mu_{33} = 0\end{gathered} \tag{7}$$

The variables λ_1, λ_2, and λ_3 correspond to ***X***, ***Y***,and ***Z*** translational DOF and λ_4, λ_5, and λ_6 correspond to ***X***, ***Y***, and ***Z*** rotational DOF, respectively.

2.3 Design of MGSP.

We used a geometry-based approach in our previous work [3,4] to obtain a closed-form expression for unknowns in 6-DOF dynamic isotropy for an MGSP. The unknows are R_{bo}, R_{to}, R_{bi}, R_{ti}, α_{to}, $(\alpha_{bi} - \alpha_{ti})$, a, Y, and H. We will extend the same geometry-based approach for 5-DOF dynamic isotropy for an MGSP. We start with one of the dynamic isotropy conditions in Eq. (7), i.e., $\lambda_1 = \lambda_2$ or $\lambda_1 = \lambda_3$, and using Eq. (6), we get:

$$b^2 = R_{ti}^2 + R_{bi}^2 - 2R_{ti}R_{bi}\cos(\alpha_{bi} - \alpha_{ti}) \tag{8}$$

where, $b^2 = \frac{H^2(3a^2+1)}{2}$. The above equation can be seen to follow the law of cosine in a triangle with sides b, R_{ti}, and R_{bi}, as shown in Fig. 3(a). Using the geometrical relationship for this triangle, the closed-form solutions to a 6-DOF isotropic MGSP were derived [3]. Using this approach, the solution of a 3-dimensional MGSP was reduced to a 2-dimensional geometry problem. To extend this to 5-DOF dynamically isotropy MGSP, the condition $\lambda_6 = 0$ (torsion mode) must be satisfied. From the expression of λ_6 in Eqs. (5) and (A1), the possible solution is:

$$\alpha_{bi} - \alpha_{ti} = 0 \text{ and } \alpha_{to} = 0 \tag{9}$$

This means that there is no relative angle between the end joints of each strut in Fig. 1. Hence, Eq. (8) reduces to

$$R_{ti} - R_{bi} = \pm H\sqrt{\frac{(3a^2+1)}{2}} = \pm b \tag{10}$$

The above equation also implies that the triangle Δocq_1 in Fig. 3(a) is now reduced to a line $\overline{oq_1c}$, as shown in Fig. 3(b). Ignoring one DOF (torsion) in MGSP simplified our geometry-based problem from 2D (triangle) to 1D (line).

Similar to Eq. (10), we can derive:

$$R_{to} - R_{bo} = \pm\frac{H}{a}\sqrt{\frac{(a^2+3)}{2}} \tag{11}$$

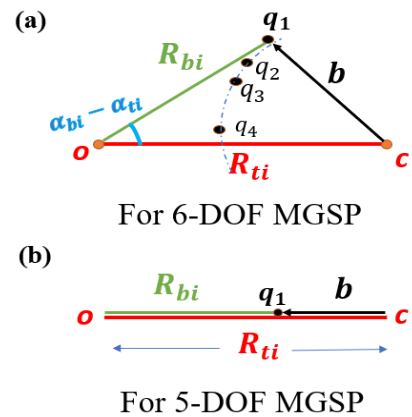

FIGURE 3: a) GEOMETRY-BASED APPROACH FOR 6-DOF DYNAMICALLY ISOTROPIC MGSP [3], b) EXTENTION TO 5-DOF DYNAMICALLY ISOTROPIC MGSP

There are four possible cases due to the $\pm$ signs in Eqs. (10) and (11). Solving transcendental equations generated using Eq. (7) for one of the cases, i.e., R_{to}<R_{bo} and R_{ti}<R_{bi}, we get

$$K_1R_{to}^2 + K_2R_{to}Y + K_3Y^2 - Q = 0 \tag{12}$$

where,

$K_1 = \frac{2a^2}{(3a^2+1)}$, $K_2 = -\frac{4a}{(3a^2+1)}\sqrt{\frac{(a^2+3)}{2}}$ and $K_3 = \frac{(a^2+3)}{(3a^2+1)}$

The determinant of the above quadratic equation is always greater than zero, indicating a real solution. However, the feasibility is ensured only when the value of the radius variable is positive. The variable Q given by $Q = I_{xx}/m_p$ is the ratio of payload's property and is known to us. For symmetrical payloads I_{xx}= I_{yy}. The solution to this equation gives two values of R_{to} shown below:

$$R_{to} = \frac{Y}{a}\sqrt{\frac{(a^2+3)}{2}} \pm \frac{\sqrt{Q}}{a}\sqrt{\frac{(3a^2+1)}{2}} \tag{13}$$

Considering the positive sign in the above equation, we get

$$R_{ti} = Y\sqrt{\frac{(3a^2+1)}{2}} - \sqrt{Q}\sqrt{\frac{(a^2+3)}{2}} \tag{14}$$

Considering the negative sign in the above equation, we get

$$R_{ti} = Y\sqrt{\frac{(3a^2+1)}{2}} + \sqrt{Q}\sqrt{\frac{(a^2+3)}{2}} \tag{15}$$

From the above formulation of R_{ti} and R_{to}, an important observation can be made that the top radii depend only on the payload's COM height (Y), payload properties (Q), and leg length ratio (a). These parameters are either known to us or can be taken as inputs. The design procedure of a 5-DOF dynamically isotropic MGSP involves:

- Select/input a, Y, and Q to find R_{to} and R_{ti} from Eqs. (13), and (14)/(15).
- Using the values of variable from the above step, we can obtain R_{bi} and R_{bo} from Eqs. (10) and (11) respectively for the case R_{to}<R_{bo} and R_{ti}<R_{bi}. The variable H (height) here can be chosen freely depending on space constraints.

The above two solutions for R_{to} or R_{ti} were for the case of R_{to}<R_{bo} and R_{ti}<R_{bi}. The other cases with their two solutions are summarized in Table 1 below. It may be noted that if any of the radius variables are negative, the solution becomes infeasible. Moreover, Table 1 is obtained for $Y > 0$, meaning the payload's COM is above the top platform (more practical case than $Y < 0$).

TABLE 1: SOLUTIONS FOR EACH POSSIBLE CASE

CASE	Condition	Sign in Eq. (12) (Quadratic equation)	Solutions ($Y > 0$)
I	$R_{to} < R_{bo}$ $R_{ti} < R_{bi}$	$K_2 < 0$	1) Feasible*
			2) Feasible*
II	$R_{to} > R_{bo}$ $R_{ti} < R_{bi}$	$K_2 > 0$	1) Feasible*
			2) Infeasible
III	$R_{to} < R_{bo}$ $R_{ti} > R_{bi}$	$K_2 < 0$	1) Feasible*
			2) Infeasible
IV	$R_{to} > R_{bo}$ $R_{ti} > R_{bi}$	$K_2 > 0$	1) Infeasible
			2) Infeasible
*Feasibility does not mean always feasible. It depends on value of payload properties and free variables (input being chosen).			

Additionally, Eq. (12) can also be seen as a pair of two parallel straight lines with R_{to} and Y as a 2-D standard basis given by

$$R_{to} - \frac{1}{a}\sqrt{\frac{(a^2+3)}{2}}\,Y \pm \frac{\sqrt{Q}}{a}\sqrt{\frac{(3a^2+1)}{2}} = 0$$

The slope for the given parallel lines, $\frac{dY}{dR_{to}} = \frac{a\sqrt{2}}{\sqrt{(a^2+3)}}$

2.4 Observation

In this subsection, we present results related to 5-DOF dynamically isotropic MGSP.

Parameter's variation

The variation of radii parameters with respect to leg length ratio for a typical payload (Q = 5.089*10^{-3} m^2, m_p = 5 Kg, Y= 75 mm), spring constant k= 10^5 N/m, and height H= 50 mm is shown in Fig. 4 for one of the feasible cases.

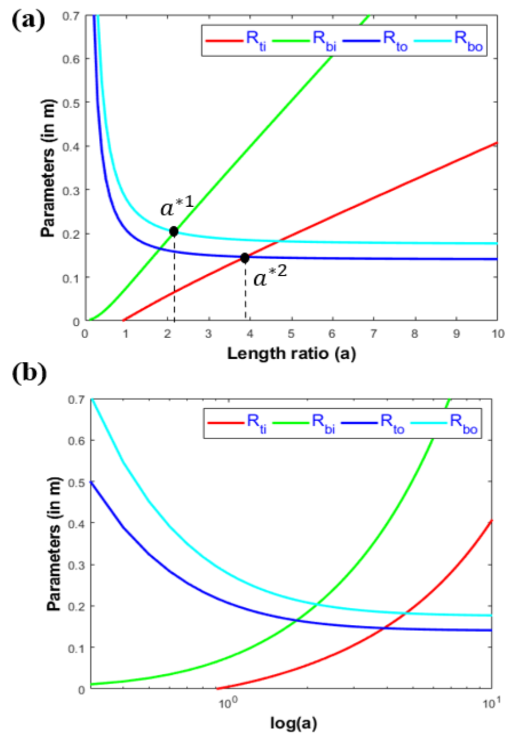

FIGURE 4. a) VARIATION OF MGSP PARAMETERS FOR $R_{to} < R_{bo}$, $R_{ti} < R_{bi}$. b) LOG PLOT FOR THE SAME

Concept of transition points ($a^{*1}$and a^{*2}).

There are two unique points denoted by $a^{*1}$and a^{*2}. At a^{*1}, both the bottom radii become equal while at a^{*2}, both the top radii become equal as shown in Fig. 4. These are named as points of transition because there is a transition from outer-to-outer radius (or inner-to-inner radius) connections to outer to inner radius connections (cross leg type) and vice versa at these points. By outer-to-outer radius connection, we mean that the outer radius of the top platform is connected to the outer radius of the bottom platform. While in the cross-leg type, the outer radius of the top platform is connected to the inner radius of the bottom platform and vice versa. This phenomenon can be visualized from Fig. 5 for the same case as in Fig. 4. The following observation can be made from Fig. 5.

- (a = 1.732) < a^{*1} → There is an outer-to-outer radius connection (or inner to inner).
- $a = a^{*1}$= 2.17 → Both the bottom radii merge to a single radius.
- a^{*1}< (a = 2.60) < a^{*2} → Transition to cross leg type connection.
- $a = a^{*2}$= 3.89 → Both the top radii merge to a single radius.
- (a = 4.20) > a^{*2} → Transition to outer-to-outer radius connection.

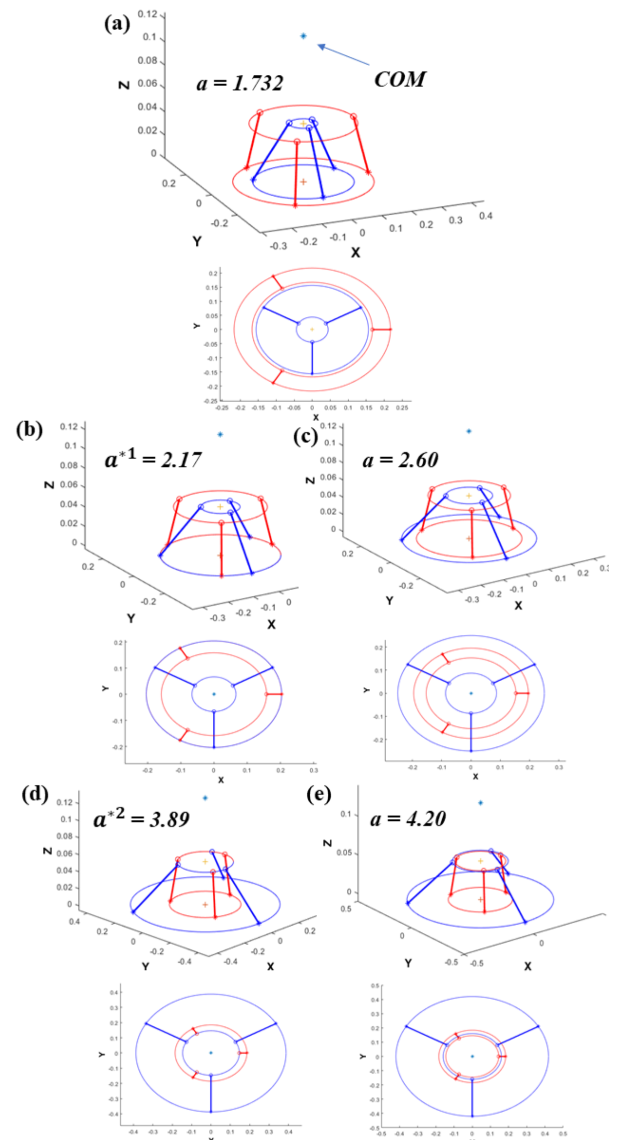

FIGURE 5: VARIOUS 5-DOF DYNAMICALLY ISOTROPIC MGSP CONFIGURATION (WITH TOP VIEWS)

Mechanical feasibility

For these configurations to be mechanically feasible, the following conditions are necessary:

- The design parameters (radius and total height) should be within our permissible limit (constraints).
- The struts do not interfere in the 3D space.

In this 5-DOF MGSP case, we have more design flexibility and control over our design than in a 6-DOF MGSP [3]. With the same payload, we can meet our design constraints in the current 5-DOF case which was not possible in 6-DOF MGSP. Moreover, there is only one possibility that the struts intersect in the 3D space in a 5-DOF case. The condition implies that there must be a cross-leg type connection and angle $\alpha_{bi} = \alpha_{ti} = 0$, as shown in Fig. 6. For any other value of $\alpha_{bi} = \alpha_{ti} = \alpha \neq 0$, the struts do not intersect. In a 6-DOF dynamically isotropy MGSP, legs are at angles ($\alpha_{bi} \neq \alpha_{ti}$ and $\alpha_{to} \neq 0$) making it more prone for interference. Therefore, a 5-DOF dynamically isotropic MGSP has more design flexibility and is more mechanically feasible than 6-DOF dynamically isotropic MGSP.

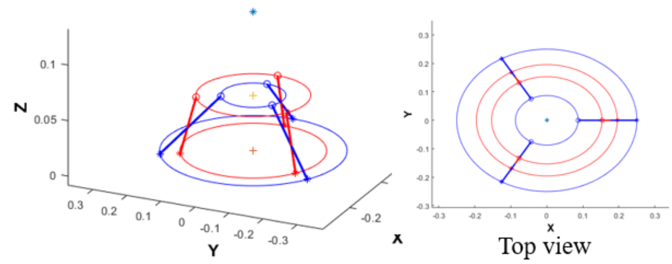

FIGURE 6: MECHANICALLY INFEASIBLE CONFIGURATION FOR 5-DOF MGSP

Natural frequency

The dynamically isotropic natural frequency will depend only on k and m_p. For the dynamic isotropy

$$\omega_1 = \omega_2 = \omega_3 = \omega_4 = \omega_5 = \sqrt{2k/m_p}. \qquad (16)$$

Hence the $[\mathbf{G}]$ matrix in Eq. (4) will be a diagonal matrix for every solution with five diagonal values as $2k/m_p$ and last torsional term as zero. The dynamically isotropic natural frequency of a 5-DOF MGSP is the same as for 6-DOF [3].

2.5 Validation

Validation of the closed-form solutions is presented in detail in Table 3 (refer to Section 5). The first five natural frequencies obtained using the FE model are very close to 31.83 Hz as obtained theoretically using $\sqrt{2k/m_p}$ which validates our design.

3. 3-DOF dynamically isotropic RPS PM.

In this section, closed-form solutions to two 3-DOF dynamically isotropic 3-3 RPS (revolute prismatic and spherical) PM is presented, one 3T (translation along ***X, Y,*** and ***Z***) type and other 2R1T (translation along ***Z*** and rotation about ***X, Y***) type. These configurations will later be superposed to generate a novel decoupled 5-DOF MGSP.

3.1 3T type 3-DOF dynamically isotropic 3-3 RPS

A typical 3-3 RPS PM has three struts with a prismatic joint connected to the bottom (fixed) platform through a revolute joint and to the top through a spherical joint as shown in Fig. 7. The variables R_{t1} and R_{b1} are the radius of the top and bottom platform, respectively. The variables H' and Y' are the platform height and payload's COM height, respectively. The angle α'_{t1} is the angle between vectors $\boldsymbol{cA_1}$ and $\boldsymbol{oB_1}$.

The same expression for $[\mathbf{B}]$ matrix as in Eq. (2) is valid here. However, j will now vary from 1 to 3. The new $[\mathbf{B}]$ matrix will be a 3×6 matrix. The new $[\mathbf{G}]$ matrix will still be a 6×6 matrix of the same form as in Eq. (5) due to the symmetricity of 120° in this case. The expressions for the new λ's and μ's (say λ'

and μ') can be referred from the appendix section at the end of this paper (see Eq. (A3)). Hence, the condition of dynamic isotropy for 3T type PM will be:

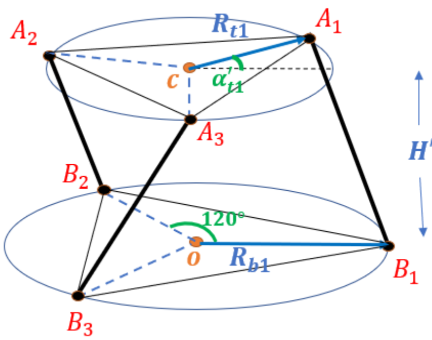

FIGURE 7*:* THE 3-3 RPS PARALLEL MANIPULATOR

$$\begin{gathered}\lambda_1' = \lambda_2' = \lambda_3' \\ \lambda_4' = \lambda_5' = \lambda_6' = 0 \text{ and } \mu_{11}' = \mu_{12}' = \mu_{13}' = 0\end{gathered} \tag{17}$$

Closed-form Solutions to this for Y'>0 is given as

$$\begin{gathered}\frac{R_{b1}}{(H' + Y')} = \frac{R_{t1}}{Y'} = \sqrt{2} \\ \text{and } \alpha_{t1}' = 0\end{gathered} \tag{18}$$

Hence, for dynamic isotropy, three struts will virtually intersect at the payload COM and with angle β= 54.74°, as shown in Fig. 8(a). We can achieve a 3T motion only at this specific arrangement of the struts. The two platform radii can lie anywhere on a cone with a semi cone angle of β= 54.74° in 3D.

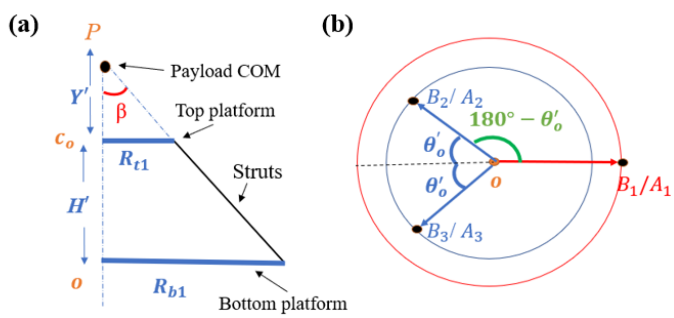

FIGURE 8: a) SIDE VIEW OF DESIGN CONE b) TOP VIEW OF 3 RPS WITHOUT ROTATIONAL SYMMETRY

3.2 3T type 3-DOF dynamically isotropic 3-3 RPS without rotational symmetry.

We consider the connection points to be on two radii on each platform for this case. The variable R_{t1} and R_{t2} are two radii of the top platform while R_{b1} and R_{b2} are two radii of the bottom platform, as shown in Fig. 8 (b). There is no rotational symmetry now and there will be many non-zero terms in the new $[\mathbf{G}]$ matrix. However, extending our observations made in section 3.1 and using the fact that the first three diagonal terms (translational modes) become equal, and the rest of the terms go to zero, for dynamic isotropy, we get

$$\begin{gathered}\frac{R_{b1}}{(H'+Y')} = \frac{R_{t1}}{Y'} = \rho \text{ and } \frac{R_{b2}}{(H'+Y')} = \frac{R_{t2}}{Y'} = \sigma \\ \sigma^2 = \frac{(2+\rho^2)}{\rho^2} \text{ and } \cos(\theta_o') = \frac{1}{\sqrt{(2+\rho^2)}}\end{gathered} \tag{19}$$

where σ and ρ are ratios (constant). The plots for this case are shown in Fig. 9. At θ_o' = 60° (previous case), $\rho = \sigma = \sqrt{2}$ and both the transition points lie at this point (i.e., R_{b1}=R_{b2} and R_{t1}=R_{t2}). Therefore, there is only an outer-to-outer radius connection, as shown in Fig. 10. The trend of parameters vs. ρ will look similar with respect to leg length ratio (a) since $a = \rho/\sqrt{2}$.

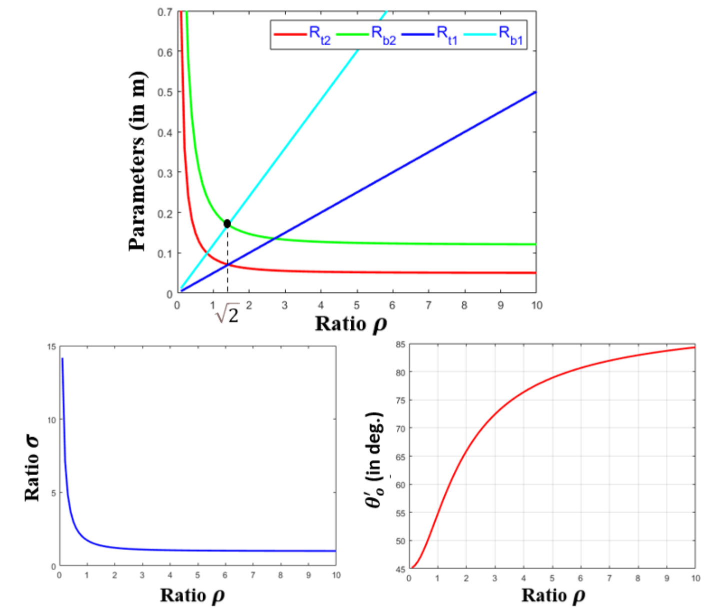

FIGURE 9: VARIATION OF PARAMETERS FOR 3T TYPE RPS

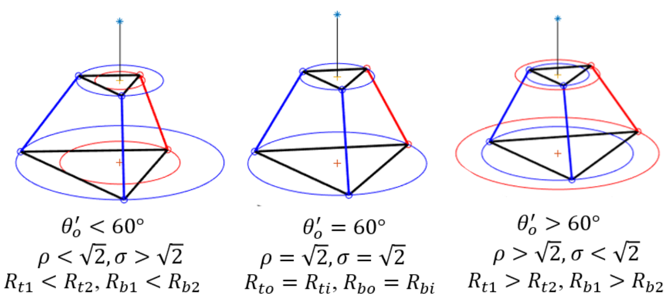

FIGURE 10: VARIOUS CONFIGURATIONS FOR 3T TYPE RPS

The $[\mathbf{G}]$ matrix and natural frequencies (ω') for dynamic isotropy in the cases discussed in Section 3.1 and 3.2 is given by:

$$\begin{gathered}[\mathbf{G}] = \text{diag}\,(k/m_p, k/m_p, k/m_p, 0, 0, 0) \\ \omega_1' = \omega_2' = \omega_3' = \sqrt{k/m_p}\end{gathered} \tag{20}$$

3.3 2R1T type 3-DOF dynamically isotropic 3-3 RPS with rotational symmetry.

For this case, the formulation remains the same as before, and terms have their usual meanings with a double prime symbol instead of a single prime for 2R1T type. The radii are now denoted as R_{t3} and R_{b3} and the condition of dynamic isotropy for the 2R1T type PM will be $\lambda_3'' = \lambda_4'' = \lambda_5''$ and other terms go to zero. For any value of $H''$and Y'', dynamic isotropy is given by:

$$R_{t3} = R_{b3} = \sqrt{2Q} = \sqrt{2I_{xx}/m_p} \text{ and } \alpha_{t3} = 0 \tag{21}$$

Therefore, the new $[\mathbf{G}]$ matrix and natural frequencies (ω'') for dynamic isotropy is given by

$$[\mathbf{G}] = \text{diag}\,(0, 0, 3k/m_p, 3k/m_p, 3k/m_p, 0)$$
$$\omega_3'' = \omega_4'' = \omega_5'' = \sqrt{3k/m_p} \tag{22}$$

3.4 2R1T type 3-DOF decoupled 3-3 RPS without rotational symmetry.

There are two radii on each platform denoted by R_{t3}, R_{b3}, R_{t4} and R_{b4} as in section 3.2. In this case, it is not possible to get a dynamic isotropic configuration except when the two radii merge to give the case with rotational symmetry (section 3.3 above). However, the new $[\mathbf{G}]$ matrix corresponding to translation $\boldsymbol{Z}$, Rot($\boldsymbol{X}$), and Rot($\boldsymbol{Y}$) can be decoupled if the following conditions are satisfied.

$$R_{t3} = R_{b3} \text{ and } R_{t4} = R_{b4}$$
$$\cos(\theta_o'') = \frac{R_{t3}}{2R_{t4}} \tag{23}$$

The variable θ_o'' holds the same meaning as θ_o' in Fig. 8(b). The effect of varying θ_o'' is shown in Fig. 11. The new $[\mathbf{G}]$ matrix for decoupled configuration is given by

$$[\mathbf{G}] = \text{diag}\left(0, 0, 3k/m_p, \frac{2R_{t4}^2 - \frac{R_{t3}^2}{2}}{I_{xx}}, \frac{3R_{t3}^2}{2I_{yy}}, 0\right) \tag{24}$$

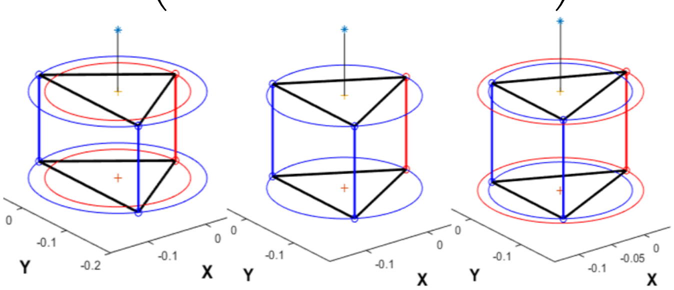

FIGURE 11: VARIOUS CONFIGURATIONS FOR 2R1T TYPE RPS

4. NOVEL 5-DOF DECOUPLED GSP.

The two 3-DOF dynamically isotropic/decoupled configurations (3T and 2R1T), as discussed in Section 3 can be geometrically superposed to obtain different decoupled 5-DOF GSP configurations. All the cases (symmetrical or unsymmetrical) satisfy analytical formulations, and the obtained $[\mathbf{G}]$ matrix is diagonal. However, a dynamically isotropic GSP (all diagonal terms of $[\mathbf{G}]$ equal) cannot be obtained by geometrical superposition. It is important to note that the height of the platform and payload's COM height in both the parent configurations must be the same. The possible combinations are presented in Table 2 where S and US represent rotational symmetric and unsymmetric configurations, respectively. When these configurations are superposed, they can be rotated with respect to each other by an angle $\boldsymbol{\varphi}$ about the $\boldsymbol{Z}$-axis depending on the parent configurations. If $\boldsymbol{p}_q'$ and $\boldsymbol{p}_q''$ are co-ordinates of anchor points of two parent configurations (3T and 2R1T), then their co-ordinate in the resulting configuration can be given by $\boldsymbol{p}_q'$ and ($[\mathbf{R_o}\,(\boldsymbol{Z}, \boldsymbol{\varphi})]\, \boldsymbol{p}_q''$). Here $[\mathbf{R_o}\,(\boldsymbol{Z}, \boldsymbol{\varphi})]$ is the rotation matrix about the $\boldsymbol{Z}$ axis. There can be two possible cases:

- The angle $\boldsymbol{\varphi}$ can hold any value→ In this case, both the parent configuration should have isotropies in $\boldsymbol{X}$ and $\boldsymbol{Y}$ as well as Rot($\boldsymbol{X}$) and Rot($\boldsymbol{Y}$). Any configuration obtained using dynamically isotropic 3T (S), 3T (US), and 2R1T (S) allow relative rotation about the $\boldsymbol{Z}$-axis. This seen be seen in Table 2 and Fig. 12.
- Angle $\boldsymbol{\varphi}$=0 or $[\mathbf{R_o}\,(\boldsymbol{Z}, \boldsymbol{\varphi})] = [\mathbf{I}]$ → Here, we cannot rotate the configurations as in the case of 2R1T (US) because it is not isotropic in Rot($\boldsymbol{X}$) and Rot($\boldsymbol{Y}$), which can be seen from $[\mathbf{G}]$ matrix in Eq. (24). Four radii GSP as shown in Fig. 13(a), is an e.g., for this case.

TABLE 2: POSSIBLE 5-DOF GSPs BY SUPERPOSITION

	Configuration 1	Configuration 2	Resulting Configuration	Relative rotation
1	3T (S)	2R1T (S)	Two radii GSP (S)	Possible
2	3T (US)	2R1T (S)	Three radii GSP (US)	Possible
3	3T (S)	2R1T (US)	Three radii GSP (US)	Not possible
4	3T (US)	2R1T (US)	Four radii GSP (US)	Not possible

Only the 3T type RPS PM contribute to translational $\boldsymbol{X}$ and $\boldsymbol{Y}$ modes, while only the 2R1T type contributes to Rot($\boldsymbol{X}$) and Rot($\boldsymbol{Y}$) modes. Therefore, only three struts can be actuated and switched accordingly for the movement required along/about any of these directions. The other three struts can remain passive. In other GSPs, all six struts need to be actuated to achieve any particular motion. This will significantly reduce power requirements, especially in spacecraft where the significance of power savings multiplies.

In these configurations upto four modes can be made equal in Case 1 and 2 in Table 2. The condition is $R_{t3} = R_{b3} = \sqrt{2Q/3}$. This gives the following decoupled natural frequencies.

$$\omega_{o1} = \omega_{o2} = \omega_{o4} = \omega_{o5} = \sqrt{k/m_p}$$
$$\omega_{o3} = \sqrt{4k/m_p} \tag{25}$$

One of these configurations is shown in Fig. 13(b) and validated in Section 5.

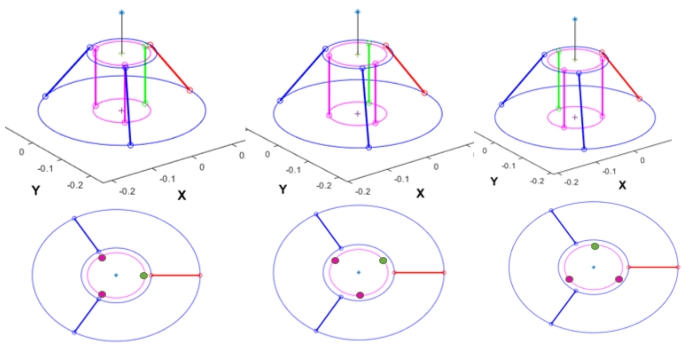

φ=0° φ= 30° φ= 90°

FIGURE 12: RELATIVE ROTATION B/W 3T AND 2R1T TYPE

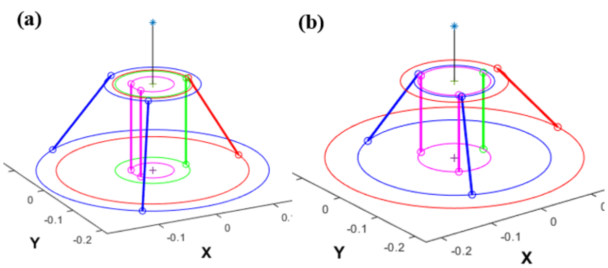

Four radii GSP **Three radii GSP**

FIGURE 13: GSPs WITHOUT ROTATIONAL SYMMETRY

5. VALIDATION THROUGH ANSYS®

Simulations were performed in ANSYS® with top and bottom platforms treated as rigid bodies and struts as ideal springs to validate the closed-form solutions in each design. The closed form solutions are compared with the Finite Element (FE) results for a typical payload with, m_p = 5 Kg, Q = 5.089*10^{-3} m^2, and k= 10^5 N/m and are summarized in Table 3. It is to be noted that the order of natural frequencies in Table 3 is translation along ***X***, ***Y***, and ***Z*** axis followed by rotation about ***X***, ***Y***, and ***Z*** axis, respectively. In each case, the closed-form solutions closely match the FE solutions for each mode which validates all the different designs presented in this paper. Any deviation from dynamically isotropic or decoupled configurations tends to deviate the natural frequency solutions from each other.

TABLE 3: COMPARISON OF RESULTS OBTAINED USING FE AND CLOSED-FORM SOLUTION

PM Type		Natural frequencies (Hz)
5-DOF MGSP in Section 2 (isotropic)	FE	31.61, 31.64, 31.79, 31.80, 31.83, ≈ 0*
	Closed form	31.83, 31.83, 31.83, 31.83, 31.83, 0
3-DOF (3T Type) in Section 3.2 (isotropic)	FE	22.50, 22.50, 22.52, ≈ 0, ≈ 0, ≈ 0
	Closed form	22.51, 22.51, 22.51, 0, 0, 0
3-DOF (2R1T Type) in Section 3.3 (isotropic)	FE	≈ 0, ≈ 0, 38.60, 38.63, 38.96, ≈ 0
	Closed form	0, 0 , 38.98, 38.98. 38.98. 0
5-DOF GSP in Section 4 (decoupled)	FE	22.44, ,22.46, 45.01, 22.50, 22.52, ≈ 0
	Closed form	22.50, 22.50, 45.01, 22.50, 22.50, 0
* ≈ 0 denotes of the order 10^{-3} Hz		

6. CONCLUSION

The use of the Gough-Stewart platform (GSP) as a 5-DOF dynamically isotropic device offer straightforward solutions, flexible design, and is more mechanical feasibility than a 6-DOF dynamically isotropic design. These features can be useful for micromotion applications where torsion or rotation about ***Z***-axis is not required. The closed-form solutions to all the geometrical parameters were developed, and points of configuration transitions were studied. The variation of the center of mass (COM) of the payload was incorporated in all our designs considering practicality. A novel 5-DOF decoupled GSP is developed using geometrical superposition of two different dynamically isotropic and decoupled 3-DOF parallel devices. Such a device does not require all six struts to be actuated for every motion and will save power and offer simpler control. Several three and five DOF asymmetrical designs without rotational symmetry were explored after extending our knowledge gained from the study of symmetrical designs. All the presented designs were validated using finite element software.

APPENDIX

For Section 2

The value of all λ's and μ's in Eq. (5) are given as:

$$\lambda_1 = \frac{3k\,(l_1^2\Psi_1 + l_2^2\Psi_2)}{2m_p l_1^2 l_2^2}, \quad \lambda_2 = \frac{3k\,(l_1^2\Psi_1 + l_2^2\Psi_2)}{2m_p l_1^2 l_2^2}, \quad \lambda_3 = \frac{3kH^2(l_1^2 + l_2^2)}{m_p l_1^2 l_2^2},$$
$$\lambda_4 = \frac{3kY^2(\,l_2^2\Psi_2 + l_1^2\Psi_1) + 6HkY\,(\Psi_3 l_1^2 + \Psi_4 l_2^2)\, + 3k\Psi_5 H^2}{2I_{xx} l_1^2 l_2^2}, \quad \lambda_5 = \lambda_4 \frac{I_{xx}}{I_{yy}},$$

$$\lambda_6 = \frac{3k(\Psi_6^2 l_1^2 + \Psi_7^2 l_2^2)}{I_{zz} l_1^2 l_2^2}\ , \ \ \mu_{11} = \frac{-3kH(-\Psi_6 l_1^2 + \Psi_7 l_2^2)}{2 l_1^2 l_2^2},$$
$$\mu_{33} = \frac{3kH(-\Psi_6 l_1^2 + \Psi_7 l_2^2)}{l_1^2 l_2^2}\ , \ \mu_{12} = \frac{3kH(\Psi_3 l_1^2 + \Psi_4 l_2^2) + 3kY(l_1^2 \Psi_1 + l_2^2 \Psi_2)}{2 l_1^2 l_2^2} \tag{A1}$$

where,

$$\Psi_1 = R_{ti}^2 + R_{bi}^2 - 2R_{ti}R_{bi}\cos(\alpha_{bi} - \alpha_{ti})$$
$$\Psi_2 = R_{to}^2 + R_{bo}^2 - 2R_{to}R_{bo}\cos(\alpha_{to})$$
$$\Psi_3 = R_{ti}^2 - R_{ti}R_{bi}\cos(\alpha_{bi} - \alpha_{ti})$$
$$\Psi_4 = R_{to}^2 - R_{to}R_{bo}\cos(\alpha_{to})$$
$$\Psi_5 = R_{ti}^2 l_1^2 + R_{to}^2 l_2^2$$
$$\Psi_6 = R_{ti}R_{bi}\sin(\alpha_{bi} - \alpha_{ti})$$
$$\Psi_7 = R_{to}R_{bo}\sin(\alpha_{to}) \tag{A2}$$

For Section 3

$$\lambda_1' = \frac{3k\Psi_1'}{2m_p l_1'^2}\ , \ \lambda_2' = \frac{3k\Psi_1'}{2m_p l_1'^2}\ , \lambda_3' = \frac{3kH'^2}{m_p l_1'^2}$$
$$\lambda_4' = \frac{3k\Psi_1' Y'^2 + 6k\Psi_3' Y' H' + 3kH'^2 R_{t1}^2}{2I_{xx} l_1'^2}\ , \ \lambda_5' = \lambda_4' \frac{I_{xx}}{I_{yy}}\ , \ \lambda_6' = \frac{3k\Psi_2'^2}{I_{zz} l_1'^2}$$
$$\mu_{11}' = \frac{-3kH'\Psi_2'}{2l_1'^2},\ \mu_{33}' = \frac{3kH'\Psi_2'}{l_1'^2},\ \mu_{12}' = \frac{3kH'\Psi_3' + 3kY'\Psi_1'}{2l_1'^2} \tag{A3}$$

where

$$\Psi_1' = R_{t1}^2 + R_{b1}^2 - 2R_{t1}R_{b1}\cos(\alpha_{t1}')$$
$$\Psi_3' = R_{t1}^2 - R_{t1}R_{b1}\cos(\alpha_{t1}')$$
$$\Psi_2' = R_{t1}R_{b1}\sin(\alpha_{t1}') \tag{A4}$$

REFERENCES

[1] J. Li, Design of 3-DOF parallel manipulators for micro-motion applications, Master's Thesis (2009).

[2] R. B. A. Shyam, N. Ahmad, R. Ranganath, A. Ghosal, Design of a dynamically isotropic Stewart-Gough platform for passive micro-vibration isolation in spacecrafts using optimization, Journal of Spacecraft Tech. 30(2) (2019) 1–8.

[3] Y. P. Singh, N. Ahmad, A. Ghosal, Design of Dynamically Isotropic Modified Gough-Stewart Platform Using a Geometry-Based Approach. Advances in Asian Mechanism and Machine Science 113 (2021) 258-268.

[4] Y. P. Singh, N. Ahmad, A. Ghosal, Design of dynamically isotropic two radii Gough-Stewart platforms with arbitrary number of struts, In: ICRoM, IEEE (2022). 66–71.

[5] H. Yun, L. Liu, Q. Li, W. Li, L. Tang, Development of an isotropic Stewart platform for telescope secondary mirror, Mechanical Systems Signal Process 127 (2019) 328–344.

[6] A. Fattah, A. M. H. Ghasemi, Isotropic design of Spatial Parallel Manipulators, International Journal of Robotics Research 21(9) (2002) 811-824.

[7] Z. Tong, J. He, H. Jiang, G. Duan, Optimal design of a class of generalized symmetric Gough-Stewart parallel manipulators with dynamic isotropy and singularity-free workspace, Robotica 30(2) (2012) 305–314.

[8] A. A. Hanieh, Active isolation and damping of vibrations via Stewart platform, ULB ASL (2003) 62-66.

[9] H. Z. Jiang, J. F. He, Z. Z. Tong, W. Wang, Dynamic isotropic design for modified Gough-Stewart platforms lying on a pair of circular hyperboloids, Mechanism and Machine Theory 46(9) (2011) 1301–1315.

[10] H. Z. Jiang, Z. Z. Tong, J. F. He, Dynamic isotropic design of a class of Gough-Stewart parallel manipulators lying on a circular hyperboloid of one sheet, Mechanism and Machine Theory 46(3) (2011) 358–374.

[11] S. Bandyopadhyay, A. Ghosal, An algebraic formulation of static isotropy and design of statically isotropic 6-6 Stewart platform manipulators, Mechanism and Machine Theory, 44 (2009) 1360-1370.

[12] Y. Yi, J. E. McInroy, F. Jafari, Generating classes of locally orthogonal Gough-Stewart platforms, IEEE Transactions on Robotics 21(5) (2005) 812–820.

[13] Y. Li, Q. Xu, Kinematic analysis and design of a new 3-DOF translational parallel manipulator, Journal of Mechanical Design Trans. ASME 128(4) (2006) 729–737.

[14] Y. Wang, C. Lyu, J. Liu, Kinematic analysis and verification of a new 5-dof parallel mechanism, Applied Sciences 11(17) (2021).

[15] X. Chen, X. Liang, Y. Deng, Q. Wang, Rigid dynamic model and analysis of 5-DOF parallel mechanism, International Journal of Advanced Robotic Systems 12 (2015) 1-9.

[16] Q. Li, Z. Huang, J. M. Hervé, Type synthesis of 3R2T 5-DOF parallel mechanisms using the lie group of displacements, IEEE Transactions on Robotics and Automation 20(2) (2004) 173–180.

[17] O. Piccin, B. Bayle, B. Maurin, M. de Mathelin, Kinematic modeling of a 5-DOF parallel mechanism for semi-spherical workspace, Mechanism and Machine Theory 44(8) (2009) 1485–1496.

[18] B. Maurin, B. Bayle, J. Gangloff, M. De Mathelin, O. Piccin, A parallel 5 DOF positioner for semi-spherical workspaces, Proc. ASME Des. Eng. Tech (2004) 1033–1042.

[19] D. Liu, R. Che, Z. Li, X. Luo, Research on the theory and the virtual prototype of 3-DOF parallel-link coordinate-measuring machine, IEEE Transactions on Instrumentation Measurement 52(1) (2003) 119–125.

[20] R. B. Ashith Shyam, A. Ghosal, Three-degree-of-freedom parallel manipulator to track the sun for concentrated solar power systems, Chinese J. Mech. Eng. 28(4) (2015).

[21] K. M. Lee, S. Arjunan, A Three-Degrees-of-Freedom Micromotion In-Parallel Actuated Manipulator, IEEE Transactions on Robotics and Automation 7(5) (1991) 634–641.